

Selected issues concerning the influence of irradiation on the characteristics of superconducting elements in modern FELs facilities

Jacek Sosnowski

National Centre for Nuclear Research, A. Soltana 7, 05-400 Otwock-Świerk, Poland

Article info

Article history:

Received 18 Oct. 2022

Received in revised form 27 Mar. 2023

Accepted 01 Apr. 2023

Available on-line 21 Apr. 2023

Keywords:

Irradiation effects; superconductors; critical current; nano-sized defects; PoFEL accelerator.

Abstract

This paper discusses issues of using superconductors in modern accelerators, such as free-electron laser type, in a radioactive environment. It shows how irradiation damages the subtle structure of superconducting materials, especially 1D and 2D high-temperature superconductors, in which it leads to the creation of nano-sized columnar-type defects. The influence of the radiation-induced structural defects on the current-carrying properties of the superconducting materials is investigated according to a developed energetic description of the capturing process on these defects, acting as pinning centres of magnetic pancake vortices. Various initial positions of the captured vortices are analysed. The influence of the irradiation-induced defects on the current-voltage characteristics is investigated, and the maximum current density is determined as a function of irradiation intensity and such physical parameters as magnetic field, temperature, and nano-defect size. This analysis is therefore of scientific interest and should also be helpful in determining the proper operating conditions of solenoids and other superconducting elements in free-electron laser facilities.

1. Introduction

In recent years, great progress has been made in the technology of nuclear accelerators, including free-electron laser (FEL)-type devices. In these facilities, superconducting materials are employed more and more frequently; recently high-temperature superconductors (HTS), as well. Superconductors are used in solenoids to generate magnetic fields, forming the electron beam at FELs and, also in current leads, resonant cavities, shields, and various correctional coils [1]. The use of superconducting materials in FELs helical, planar, or staggered array undulators constructions made of bulk HTS materials is very promising, as well [2]. Despite the great advantages of using these materials with formally zero resistance, particular problems arise within nuclear accelerating machines, due to their behaviour in a radioactive environment. This paper addresses issues arising while using superconductors in the irradiation environment of modern accelerators. An analysis of the effects of irradiation on the

subtle structure of the superconductors, including 1D and 2D structures of HTS materials in which columnar defects are then created is presented in the paper. The potential energy approach, describing the interaction of magnetic vortices with irradiation-generated defects, is then analysed. This model can also be used to describe the function of defects arising during the winding procedure of superconducting coils. The relevance of the issue of capturing magnetic vortices in superconductors is indicated by the large number of papers prepared in this area, some of which are for instance given in Refs. 3–10.

2. Energetic approach to irradiation issues in superconductors

It is intuitively expected that irradiation of superconducting materials will lead to variation of their physical properties. It concerns especially the low dimensional superconductors, such as 2D CuO₂-based HTS: REBaCuO (RE means rare earth) and BiSrCaCuO composites. Effect of irradiation is especially true for quasi 1D A15-type superconductors, whose structure is characterised by the

*Corresponding author at: jacek.sosnowski@ncbj.gov.pl

existence of three perpendicular linear chains of the transition metals atoms. The most well-known representative of this class is Nb₃Sn because this compound is used for fabrication of superconducting wires. Irradiation of these materials, occurring in acceleration devices, will lead to disruption of the chains responsible for their superconducting properties, as shown in Fig. 1.

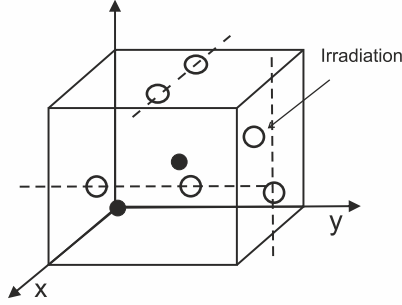


Fig. 1. Deformation of the crystal structure of the A15-type superconductor irradiated by fast neutrons: (○) – transition metal atoms (Nb, V) forming linear chains, (●) – non-transition metal atoms (Sn, Ga).

Despite these problems, superconducting materials are more and more attractive from the point of view of their application in nuclear physics devices. Especially promising are HTS due to a continuous increase of the critical temperature now even reaching almost room temperature. Beside magnets already working commercially in numerous laboratories of scientific establishments and in nuclear magnetic resonance (NMR) in hospitals, nuclear accelerators using superconducting materials are currently being constructed or modernised. Superconducting elements also form a very important part of FELs linear accelerators. In these constructions, the superconducting materials are exposed to nuclear irradiation by the primary ionic beam, or, as in the case of FELs, by both initial electron beam and secondary irradiation beam composed of photons, neutrons, and ions.

The influence of the nano-sized defects, caused by irradiation, on the superconducting materials properties is investigated based on the general equation describing the energy [11] of a system of N -magnetic vortices of the pancake type, characteristic of multi-layered HTS, captured on pinning centres

$$\begin{aligned}
 &F(r_1, \dots, r_N) \\
 &= \sum_{i=1}^N U(r_i) + \frac{1}{2} \sum_{i \neq j}^N F_{inter}(r_i - r_j) \\
 &- J\Phi_0 l \cdot \sum_{i=1}^N (l_i - r_i) - \sum_{i=1}^N \frac{C(r_i - \xi)^2}{2} V_i.
 \end{aligned} \tag{1}$$

In (1), r_i denotes the position of the vortex captured on the nano-defect created by the ionizing irradiation. U is the pinning potential of the captured pancake vortex, while summation runs over each of N -captured magnetic vortices. F_{inter} , in the second term, denotes the interaction energy between magnetic vortices placed in positions r_i and r_j . Third factor concerns the Lorentz force contribution to the potential energy, proportional to the deflection l_i of vortex from the captured position r_i , caused by the Lorentz

interaction of the flowing electric current of density J with the magnetic quantized flux $\Phi_0 = 2.07 \cdot 10^{-15}$ Wb transported by each vortex. l is the thickness of the superconducting layer, while ξ is the coherence length. The last component in (1) gives the elasticity energy of the vortex lattice, deformed during the shift of the vortex from equilibrium position at the process of the magnetic flux capturing. V_i describes the volume of the deformed lattice, while C is the spring constant of the vortex lattice, proportional to the elasticity parameter α_e appearing in (5). Movement of the vortex in the flux creep process against the initial position of the half-captured pancake vortex, shown in Fig. 2, leads to an enhancement of the normal state volume and potential energy increase, which is described by (2) for that case. However, other initial captured vortex states, such as fully pinned pancake vortex, shown in Fig. 3, were studied, too.

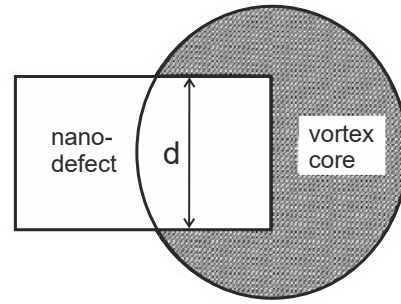


Fig. 2. Schematic view of the half-captured vortex core on the pinning centre of the width d .

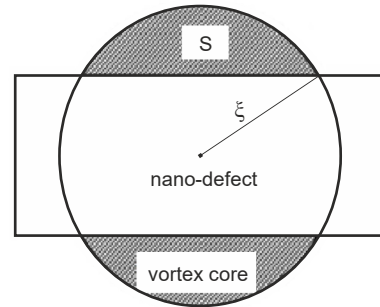


Fig. 3. Configuration of the fully captured pancake vortex core of the area S and the radius of the coherence length ξ inside a thin rectangular nano-defect.

This configuration is preferred for smaller defect dimensions, created especially by low energy electrons irradiation. Equation (2) describes the change of the potential energy $U(x)$ for a vortex moving on distance x , lower than critical deflection x_c

$$U_1(x) = \frac{\mu_0 H_c^2 l}{2} \left(dx - \xi^2 \arcsin \frac{d}{2\xi} - \frac{d\xi}{2} \sqrt{1 - \left(\frac{d}{2\xi}\right)^2} \right), \tag{2}$$

while for larger vortex deflections from the initial position at the rectangular defect of the width d , potential energy is

$$U_2(x) = \frac{\mu_0 H_c^2 l}{2} \left(x\xi \sqrt{1 - \left(\frac{x}{\xi}\right)^2} - \xi^2 \arcsin \sqrt{1 - \left(\frac{x}{\xi}\right)^2} \right). \tag{3}$$

In (2)–(3), H_c is the thermodynamic critical magnetic field.

Existence of the potential energy $U(x)$ varying with the vortex deflection from the initial position, against the irradiation-created capturing centre, under current flow according to the Lorentz force, leads to the creation of a potential barrier ΔU . This barrier, given by (4) in the Cartesian coordination system, should pass vortex in a flux creep process, which is a thermally activated flux movement between nearest capturing centres, preceding the flux flow

$$\begin{aligned} \Delta U(x_m) &= \frac{\mu_0 H_c^2}{2} l \xi^2 \left(\arcsin \frac{x_m}{\xi} - \frac{\pi}{2} + \arcsin \left(\frac{d}{2\xi} \right) \right. \\ &\quad \left. + \frac{x_m}{\xi} \sqrt{1 - \left(\frac{x_m}{\xi} \right)^2} + \frac{d}{2\xi} \sqrt{1 - \left(\frac{d}{2\xi} \right)^2} \right) - JB\pi \xi^2 l x_m. \end{aligned} \quad (4)$$

In (4), x_m is the value of the vortex shift against the initial position in capturing defect, at a distance for which the potential barrier reaches the maximum. Potential barrier $\Delta U(i)$ in current representation is

$$\begin{aligned} \Delta U(i) &= \frac{\mu_0 H_c^2}{2} l \xi^2 \left(-\arcsin(i) + \arcsin \left(\frac{d}{2\xi} \right) + \frac{d}{2\xi} \sqrt{1 - \left(\frac{d}{2\xi} \right)^2} \right. \\ &\quad \left. - i \left[\sqrt{1 - i^2} + \arcsin \left(\frac{d}{2\xi} \right) + \frac{d}{2\xi} \sqrt{1 - \left(\frac{d}{2\xi} \right)^2} - \frac{\pi}{2} \right] \right) \\ &\quad + \frac{\xi^2 \sqrt{1 - i^2}}{\xi} (\sqrt{1 - i^2} - 2) \alpha_e. \end{aligned} \quad (5)$$

The last term in (5) corresponds to the elasticity properties of the vortex lattice, characterised by the elasticity parameter α_e , while $i = j/j_c$, where j is the transport current density, and j_c is the critical current density.

3. Current-voltage characteristics analysis

The analysed above potential barrier height ΔU has a crucial meaning for determining the current-voltage characteristics (I - V curves) and the critical current density j_c of the superconducting materials. To that end, we have used (6) describing the generated electric field E for the forward and backward flux creep processes, as a function of the reduced to critical transport current density $i = j/j_c$

$$E = -B\omega h \left(\exp \left(\frac{-\Delta U(0)(1+i)}{k_B T} \right) - \exp \left(\frac{-\Delta U(i)}{k_B T} \right) \right). \quad (6)$$

In (6), B is the applied magnetic induction, h is the distance between the nearest capturing pinning centres created by irradiation, ω is the creep process frequency, k_B is the Boltzmann's constant, T is the temperature. Results of calculations [12] of the current-voltage characteristics fitted to the experimental data measured at liquid nitrogen temperature on the prepared superconducting sample of the composition of BiPbSrCaCuO vs. applied steady magnetic

field are shown in Fig. 4. This comparison indicates good agreement and confirms the validity of the presented model, which can, therefore, also be useful for characterisation of superconducting wires in FELs accelerators. For instance, the concentration of radiation-created defects can thus be deduced from this fitting procedure and the variation of the critical current under irradiation in a static magnetic field can be theoretically investigated, as it will be shown in the next section.

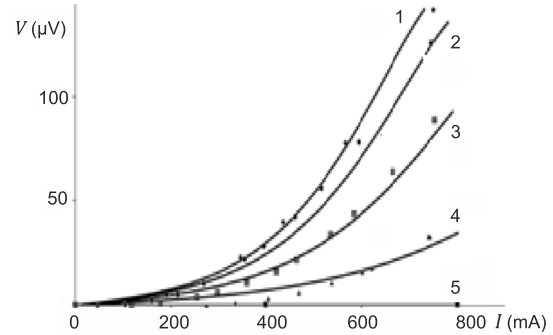


Fig. 4. Comparison (according to Ref. 12) of fitting theoretical model (·) to the experimental I - V characteristics measured on a prepared superconducting sample of BiPbSrCaCuO composition, for various steady magnetic fields: (1) $B = 35$ mT, (2) $B = 33$ mT, (3) $B = 24$ mT, (4) $B = 13.5$ mT, (5) $B = 0$ mT at $T = 77$ K.

The theoretical approach presented is also applicable for dynamically varying magnetic fields, predicting the appearance of anomalies in dynamic current-voltage characteristics, which have been previously observed experimentally [13]. In this experiment, a flat superconducting sample, through which a direct current flows, was inserted into a perpendicular slowly varying magnetic field and the measured electric field E . The dynamic anomalies were then observed being the function of the current and its frequency, as well as of the magnetic field sweep rate. Figure 5 shows a theoretically calculated dependence of these anomalies on the magnetic field sweep rate, indicating the possibility of applying them as superconducting sensors to measure a magnetic field variation. Also, the shape of anomalies depends on the quality of the superconductor and on the velocity of the magnetic flux diffusion into it, the properties of which can also be interesting from the point of view of sensor application.

The nano-defects in the superconducting elements used in FELs accelerators are created as the result of irradiation, which case is described by the present theoretical approach.

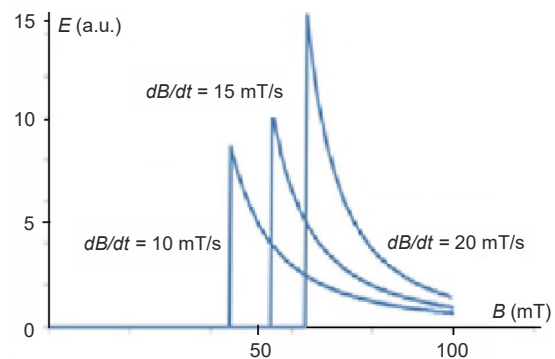


Fig. 5. Calculated dynamic anomalies of the electric field E vs. induction B , generated in a slowly varying magnetic field for HTS materials.

These defects are also created during the winding procedure of superconducting magnets used in accelerators. As a result of a subsequent bending strain, micro-cracks and dislocations are created which interact with vortices as is described in this model. The analysis has considered the variation of the critical current in deformed by bending strain regions, due to the change in cross-section of the superconducting wires then.

4. Influence of irradiation on critical current density

The energetic approach-based model, presented in the previous section, leads to a description of the current-voltage characteristics of the superconducting materials. Also, the model allows a subsequent determination of the critical current densities of superconducting elements, such as tapes appearing in FELs-type superconducting accelerators, and their dependence on the irradiation dose. The results of numerical calculations of critical current density dependence on temperature, magnetic field, and irradiation-created nano-defects size are presented in Figs. 6–8. These results indicate that initially, with a small irradiation dose, an enhancement of critical current density appears, due to increase of pinning interaction, reaching finally the maximum, while for higher irradiation intensity, the destruction of the crystal lattice prevails, and critical current starts to decrease.

The effect predicted here of a decrease in critical current density for a high irradiation dose, connected with damage of the superconductor structure in accelerators, is in general agreement with the experimental data concerning the materials used in nuclear reactors. High flux densities of fast neutrons lead then to a serious radiation damage and even so-called "irradiation-induced swelling" of the materials [14]. The voids in the structure are created while their aggregation leads to a substantial increase in the material volume and a deterioration of its mechanical, and in the case of wires, superconducting properties.

Thus, from the applied point of view, it is important to fit the working conditions of a given superconducting accelerating machine to the irradiation range generated in this construction.

Experimentally, it is indeed observed that not too intensive nuclear irradiation, leading to an increase in the concentration of capturing centres, will enhance the critical current. Such an effect has been experimentally detected during irradiation of HTS by heavy ions for an optimal surface concentration of about 10^{11} – 10^{12} cm^{-2} , losing energy of $dE/dx = 5$ – 10 keV/nm, or electrons and neutrons of energy $E > 0.1$ MeV and light ions losing energy of $dE/dx < 2$ – 5 keV/nm. Thus, it corresponds just to the case shown in Figs. 6–8. Also, fast neutrons of a concentration higher than 10^{18} cm^{-2} and energy higher than $E > 1.4$ MeV enhance the critical current of HTS doped with U^{238} uranium atoms, artificially inserted. Irradiation of U-doped HTS samples by these neutrons causes the decay of uranium atoms and then the creation of new pinning centres. Other artificial methods are sometimes also used to create new pinning centres inside HTS, e.g., by bombarding the heavy atoms of BiPbSrCaCuO and HgBaCuO materials by protons or deuterium atoms of energy in the range of 200–1000 MeV, leading to their fission and increase of j_c .

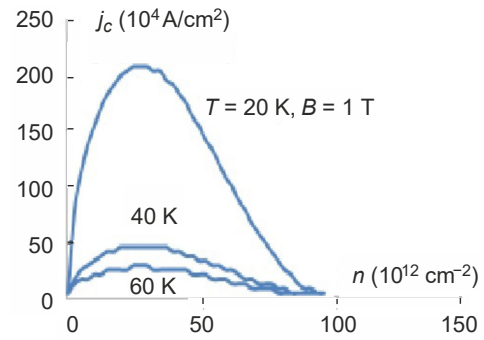


Fig. 6. The influence of temperature on the theoretically predicted critical current density as a function of irradiation intensity.

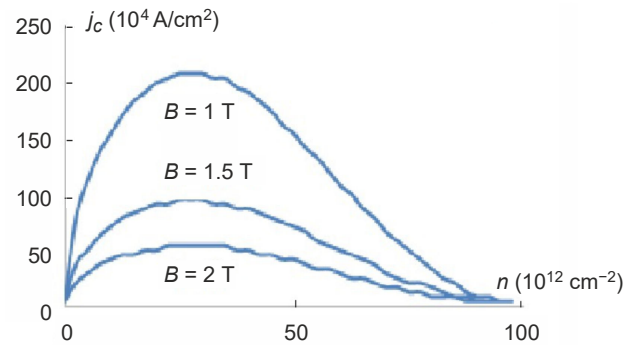


Fig. 7. The influence of the magnetic induction on the theoretically predicted critical current density as a function of irradiation dose.

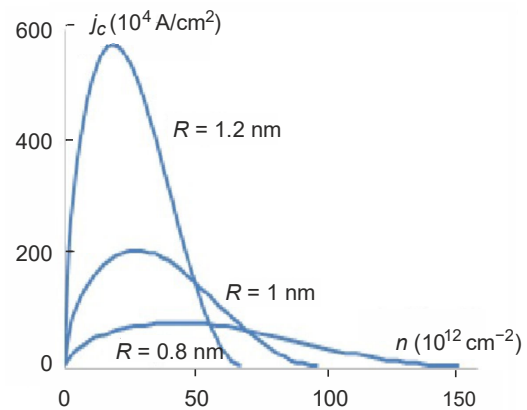


Fig. 8. The dependence of the critical current density of the superconducting material on the irradiation dose as a function of nano-defects size R .

5. Conclusions

This paper has presented a phenomenological approach describing the influence of irradiation, and resulting nano-dimensional defects, on the critical currents phenomena in superconducting materials. These issues are, therefore, tightly connected with FELs facilities, in which alongside electrons beam, photonic irradiation, as well as secondary neutrons, positrons, and γ -rays beams also appear. These beams interact with superconducting elements, such as wires in solenoids, current leads, and resonant cavities. The existence of the maximum value of the critical current density under appropriate irradiation dose and its subsequent decrease have been discussed in the paper.

References

- [1] Sosnowski, J. *Superconducting Cryocables*. (Book Publisher of Electrotechnical Institute, 2012). (In Polish)
- [2] Zhang, K. & Calvi, M. Review and prospects of world-wide superconducting undulator development for synchrotrons and FELs. *Supercond. Sci. Technol.* **35**, 3001 (2022). <https://doi.org/10.1088/1361-6668/ac782a>
- [3] Cho, K. *et al.* Intermediate scattering potential strength in electron-irradiated YBa₂Cu₃O_{7-δ} from London penetration depth measurements. *Phys. Rev. B* **105**, 014514 (2022). <https://doi.org/10.1103/PhysRevB.105.014514>
- [4] Blatter, G., Ivlev, B. & Vinokur, V. Quantum depinning of vortices in type-II superconductors. *Phys. Rev. B Condens. Matter. Matter. Phys.* **54**, 13330–13338 (1996). <https://doi.org/10.1103/physrevb.54.13330>
- [5] Kwok, W-K. *et al.* Vortices in high-performance high-temperature superconductors. *Rep. Prog. Phys.* **79**, 116501 (2016). <https://doi.org/10.1088/0034-4885/79/11/116501>
- [6] Zeldov, E. *et al.* Thermodynamic observation of first-order vortex-lattice melting transition in Bi₂Sr₂CaCu₂O₈. *Nature* **375**, 373–376 (1995). <https://doi.org/10.1038/375373a0>
- [7] Brandt, E. H. Vortices in superconductors: ideal lattice, pinning, and geometry effects. *Supercond. Sci. Technol.* **22**, 034019 (2009). <https://doi.org/10.1088/0953-2048/22/3/034019>
- [8] Nabialek, A. *et al.* Annealing of defects in fast neutron irradiated YBa₂Cu₃O_x ceramics magnetic and microwave studies. *Physica C Supercond.* **226**, 345–352 (1994). [https://doi.org/10.1016/0921-4534\(94\)90215-1](https://doi.org/10.1016/0921-4534(94)90215-1)
- [9] Van Bael, M. J., Lange, M., Van Look, L., Moshchalkov, V. V. & Bruynseraede, Y. Vortex pinning in ferromagnet/superconductor hybrid structures, *Physica C* **364–365**, 491–494 (2021). [https://doi.org/10.1016/S0921-4534\(01\)00829-2](https://doi.org/10.1016/S0921-4534(01)00829-2)
- [10] Wimbush, S. C., Durrell, J. H., Blamire, M. & MacManus-Driscoll, J. Strong flux pinning by magnetic interlayers compatible with YBa₂Cu₃O_{7-δ}. *IEEE Trans. Appl. Supercond.* **21**, 3159–3161 (2011). <https://doi.org/10.1109/TASC.2010.2097574>
- [11] Sosnowski, J. New model of the pinning potential barrier in layered HTc superconductors. *Mod. Phys. Lett. B* **30**, 1650387 (2016) <https://doi.org/10.1142/S0217984916503875>
- [12] Sosnowski, J. New approach to pancake vortices interaction with nanosized defects in HTc superconductors. *Mod. Phys. Lett. B* **28**, 1450132 (2014). <https://doi.org/10.1142/S0217984914501322>
- [13] Sosnowski, J. & Datskov, V. I. Normal and inverse anomaly of dynamic current-voltage characteristics of high *T_c* oxide superconductors. *Cryogenics* **33**, 108–112 (1993). [https://doi.org/10.1016/0011-2275\(93\)90086-4](https://doi.org/10.1016/0011-2275(93)90086-4)
- [14] Edwards, D. J., Garner, F. A. & Gelles, D. S. The influence of neutron irradiation in FFTF on the microstructural and micro-chemical development of Mo–41Re at 470–730 °C. *J. Nucl. Mater.* **375**, 370–381 (2008). <https://doi.org/10.1016/j.jnucmat.2008.01.014>